Selective Synthesis of Single-Crystalline Selenium Nanobelts and Nanowires in Micellar Solutions of Nonionic Surfactants

Yurong Ma, Limin Qi,* Wei Shen, and Jiming Ma

State Key Laboratory for Structural Chemistry of Unstable and Stable Species, College of Chemistry, Peking University, Beijing 100871, PR China

Received March 26, 2005. In Final Form: May 27, 2005

Single-crystalline nanobelts and nanowires of trigonal selenium (t-Se) have been selectively synthesized in micellar solutions of nonionic surfactants. In particular, t-Se nanobelts about 30 nm in thickness were obtained in micellar solutions of poly(oxyethylene(20)) octadecyl ether ($C_{18}EO_{20}$), whereas t-Se nanowires were obtained in micellar solutions of poly(oxyethylene(10)) dodecyl ether ($C_{12}EO_{10}$). The obtained t-Se nanobelts exhibit a low-energy absorption peak that is considerably red shifted from that for t-Se nanowires, which has been presumably attributed to the lower degree of crystal perfection for the t-Se nanobelts with rectangular cross sections.

Introduction

The controlled synthesis of 1D nanostructures, such as nanotubes, nanowires, nanorods, and nanobelts, has been the focus of extensive research owing to their unique physical and chemical properties and potential applications in the fabrication of nanoscale devices.[1] In particular, nanobelts (or nanoribbons), a relatively new family of 1D nanostructures with a rectangular cross section, have received increasing attention since the discovery of novel oxide semiconductor nanobelts.[2] A variety of functional oxide[3] and sulfide[4] nanobelts have been successfully fabricated by simple thermal evaporation. Meanwhile, many efforts have been devoted to the exploration of low-temperature solution routes to inorganic nanobelts considering that a mild solution synthesis would be desirable in terms of low cost and large-scale production. For example, nanobelts of vanadium pentoxide,[5a] lithium manganese oxide,[5b] bismuth oxide bromide,[5c] ZnS,[5d] and tellurium[5e] have been prepared by hydrothermal/solvothermal methods, whereas $CdWO_4$ [6a] and $BaCrO_4$ [6b] nanobelts have been produced by a double-jet crystallization process and a reverse micelle-mediated synthesis, respectively. However, it remains a great challenge to develop facile and mild solution approaches to nanobelts of various functional materials.

Selenium is an important elemental semiconductor with many interesting properties including a relatively low melting point (~490 K), high photoconductivity (~8×10^4 S cm^{-1}), and nonlinear optical responses, hence it has found widespread applications in various areas such as photovoltaic cells, rectifiers, photographic exposure meters, and xerography.[7] Moreover, selenium has a high reactivity toward a variety of chemicals, which can be potentially explored to transform selenium into many other functional materials through template-engaged reactions.[8] In addition, trigonal selenium (t-Se) contains infinite spiral chains of Se atoms along the *c* axis, which makes t-Se an ideal candidate for generating 1D nanostructures without the assistance of templates. A number of methods have been demonstrated for generating t-Se nanowires and nanorods; notable examples include the reduction of selenious acid by solution refluxing[9] or sonochemical approaches,[10] solution-mediated transformation from Se powder[11] or stabilizer-depleted CdSe nanoparticles,[12] and an evaporation and condensation process from Se powder.[13] However, there have been only limited reports on the controlled synthesis of t-Se nanobelts and nanotubes.[14,15] It is noteworthy that ultrathin t-Se nanoribbons with zigzag edges have been fabricated by a direct vapor deposition process.[14] Recently, we reported the synthesis of t-Se nanotubes by the dismutation of Na_2SeSO_3 in micellar solutions of the nonionic surfactant poly(oxyethylene(23)) dodecyl ether ($C_{12}EO_{23}$).[15a] We also found that a mixture consisting of a small number of Se nanobelts

* Corresponding author. E-mail: liminqi@pku.edu.cn.

(1) (a) Hu, J.; Odom, T. W.; Lieber, C. M. *Acc. Chem. Res.* **1999**, *32*, 435. (b) Xia, Y.; Yang, P.; Sun, Y.; Wu, Y.; Mayers, B.; Gates, B.; Yin, Y.; Kim, F.; Yan, H. *Adv. Mater.* **2003**, *15*, 353. (c) Wang, Z. L. *Annu. Rev. Phys. Chem.* **2004**, *55*, 159.

(2) Pan, Z. W.; Dai, Z. R.; Wang, Z. L. *Science* **2001**, *291*, 1947.

(3) (a) Wang, Z. L. *Adv. Mater.* **2003**, *15*, 432. (b) Dai, Z. R.; Pan, Z. W.; Wang, Z. L. *Adv. Funct. Mater.* **2003**, *13*, 9.

(4) (a) Ma, C.; Moore, D.; Li, J.; Wang, Z. L. *Adv. Mater.* **2003**, *15*, 228. (b) Jiang, Y.; Meng, X.-M.; Liu, J.; Xie, Z.-Y.; Lee, C.-S.; Lee, S.-T. *Adv. Mater.* **2003**, *15*, 323. (c) Gong, J.; Yang, S.; Duan, J.; Zhang, R.; Du, Y. *Chem. Commun.* **2005**, 351.

(5) (a) Liu, J.; Wang, X.; Peng, Q.; Li, Y. *Adv. Mater.* **2005**, *17*, 764. (b) Zhang, L.; Yu, J. C.; Xu, A.-W.; Li, Q.; Kwong, K. W.; Wu, L. *Chem. Commun.* **2003**, 2910. (c) Wang, J.; Li, Y. *Chem. Commun.* **2003**, 2320. (d) Yao, W.-T.; Yu, S.-H.; Pan, L.; Li, J.; Wu, Q.-S.; Zhang, L.; Jiang, J. *Small* **2005**, *1*, 320. (e) Mo, M.; Zeng, J.; Liu, X.; Yu, W.; Zhang, S.; Qian, Y. *Adv. Mater.* **2002**, *14*, 1658.

(6) (a) Yu, S.-H.; Antonietti, M.; Cölfen, H.; Giersig, M. *Angew. Chem., Int. Ed.* **2002**, *114*, 2462. (b) Shi, H.; Qi, L.; Ma, J.; Cheng, H.; Zhu, B. *Adv. Mater.* **2003**, *15*, 1647.

(7) (a) *Selenium*; Zingaro, R. A., Cooper, W. C., Eds.; Van Nostrand Reinhold: New York, 1974. (b) Berger, L. I. *Semiconductor Materials*; CRC Press: Boca Raton, FL, 1997; p 86.

(8) (a) Gates, B.; Wu, Y.; Yin, Y.; Yang, P.; Xia, Y. *J. Am. Chem. Soc.* **2001**, *123*, 11500. (b) Jiang, X.; Mayers, B.; Herricks, T.; Xia, Y. *Adv. Mater.* **2003**, *15*, 1740. (c) Mayers, B.; Jiang, X.; Sunderland, D.; Cattle, B.; Xia, Y. *J. Am. Chem. Soc.* **2003**, *125*, 13364.

(9) (a) Gates, B.; Yin, Y.; Xia, Y. *J. Am. Chem. Soc.* **2000**, *122*, 12582. (b) Gates, B.; Mayers, B.; Cattle, B.; Xia, Y. *Adv. Funct. Mater.* **2002**, *12*, 219.

(10) (a) Gates, B.; Mayers, B.; Grossman, A.; Xia, Y. *Adv. Mater.* **2002**, *14*, 1749. (b) Mayers, B. T.; Liu, K.; Sunderland, D.; Xia, Y. *Chem. Mater.* **2003**, *15*, 3852.

(11) Cheng, B.; Samulski, E. T. *Chem. Commun.* **2003**, 2024.

(12) Tang, Z.; Wang, Y.; Sun, K.; Kotov, N. A. *Adv. Mater.* **2005**, *17*, 358.

(13) (a) Cao, X.; Xie, Y.; Li, L. *Adv. Mater.* **2003**, *15*, 1914. (b) Ren, L.; Zhang, H.; Tan, P.; Chen, Y.; Zhang, Z.; Chang, Y.; Xu, J.; Yang, F.; Yu, D. *J. Phys. Chem. B* **2004**, *108*, 4627.

(14) Cao, X.; Xie, Y.; Zhang, S.; Li, F. *Adv. Mater.* **2004**, *16*, 649.

(15) (a) Ma, Y.; Qi, L.; Ma, J.; Cheng, H. *Adv. Mater.* **2004**, *16,* 1023. (b) Zhang, H.; Yang, D.; Ji, Y.; Ma, X.; Xu, J.; Que, D. *J. Phys. Chem. B* **2004**, *108*, 1179.

10.1021/la050801l CCC: $30.25
Published on Web 06/09/2005

and a large number of Se nanowires was obtained in the synthesis system under suitable conditions. Herein, we demonstrate that the selective synthesis of Se nanobelts and nanowires can be realized by using micellar solutions of selected nonionic surfactants. Single-crystalline t-Se nanobelts (about 30 nm in thickness) showing smooth edges have been obtained in micellar solutions of poly(oxyethylene(20)) octadecyl ether ($C_{18}EO_{20}$). To the best of our knowledge, this is the first report on a facile solution synthesis of single-crystalline t-Se nanobelts.

Experimental Section

Selenium nanobelts and nanowires were selectively synthesized by the dismutation of Na_2SeSO_3 under acidic condition in aqueous micellar solutions of nonionic surfactants $C_{18}EO_{20}$ (Brij 78, Sigma) and $C_{12}EO_{10}$ (poly(oxyethylene(10)) dodecyl ether, Sigma), respectively, following the procedure reported for the micelle-mediated synthesis of Se nanotubes.[15a] Typically, 0.4 mL of 0.2 M Na_2SeSO_3 was added to 4.2 mL of acidic solution containing acetic acid (HAc, 0.2 mmol) and 0.025 g of $C_{18}EO_{20}$ (or $C_{12}EO_{10}$), resulting in the immediate appearance of red color in the solution, which indicated the formation of amorphous selenium (a-Se).[9] The mixture was sonicated for 3 h in a normal ultrasonic bath (Branson SB3200, 40 kHz), which was accompanied by an increase in temperature up to ~50 °C and a gradual color change from red to brown and cloudy, indicating a transformation from less stable a-Se to stable t-Se. The resulting solution was further aged for 2 h in darkness at room temperature, and the solid product was collected by centrifugation. It may be noted that although the sonication process accelerated the formation of 1D selenium products it was not a necessary condition and similar products could also be obtained without sonication but at higher thermostated temperatures (e.g., 80 °C), similar to the situation of the Se nanotubes reported previously.[15a] The final products were characterized by scanning electron microscopy (SEM, FEI STRATA DB235), transmission electron microscopy (TEM, JEOL JEM 200CX), high-resolution TEM (HRTEM, FEI TECNAI F30), powder X-ray diffraction (XRD, Rigaku Dmax-2000), and UV−vis (Shimadzu UV-250) and Raman spectra (Renishaw 1000).

Results and Discussion

Figure 1a presents a representative low-magnification SEM image of the selenium product obtained in $C_{18}EO_{20}$ micellar solution, which suggests that the product shows exclusive wirelike morphology with lengths ranging from several micrometers to more than 100 μm. The corresponding XRD pattern (Figure 2a) exhibits reflections characteristic of the trigonal phase of selenium (JCPDS file no. 6-362), and the related energy-dispersive X-ray spectroscopy (EDS) spectrum (Figure 2b) suggests that the product is composed of pure selenium. The abnormally intensified (100) peak in the XRD pattern also indicates that the wirelike product comprises 1D t-Se crystals preferentially grown along the [001] direction. Typical high-magnification SEM images of the wirelike product (Figure 1b and c) reveal that the product actually consists of Se nanobelts typically ranging from 100 to 300 nm in width and around 30 nm in thickness. All of the nanobelts exhibit sharp edges, and their flexibility does not seem to be high because the bending of the nanobelts has seldom been observed and the breaking of the nanobelts can be observed occasionally (Figure 1c). It is indicated that the current Se nanobelts are different from the flexible, ultrathin Se nanobelts (~15 nm in thickness) with zigzag edges obtained by the vapor deposition process.[14] A typical TEM image of the obtained Se nanobelts is presented in Figure 1d, which clearly shows the bending of a nanobelt, confirming a beltlike morphology. Figure 1e shows a single nanobelt as well as its electron diffraction (ED) pattern, which indicates that the whole nanobelt is a single crystal

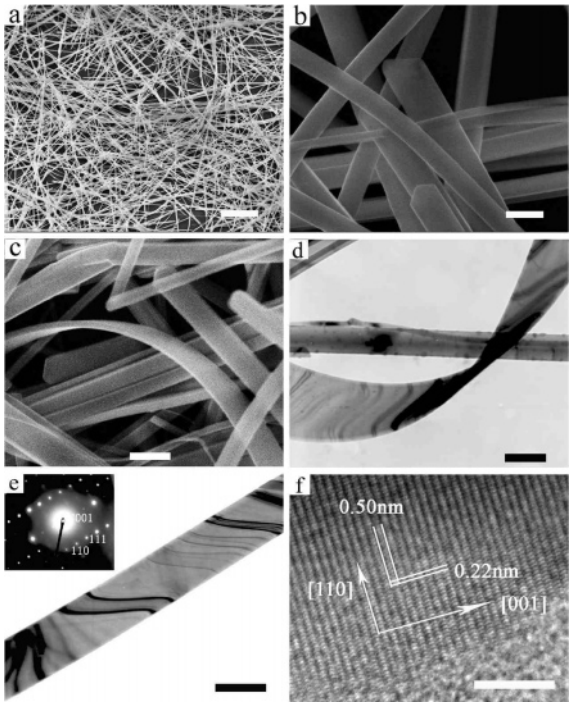

Figure 1. SEM (a−c), TEM (d−e), and HRTEM (f) images of Se nanobelts obtained in $C_{18}EO_{20}$ micellar solution. The inset shows the related ED patten. Scale bars: (a) 5 μm, (b−e) 200 nm, and (f) 5 nm.

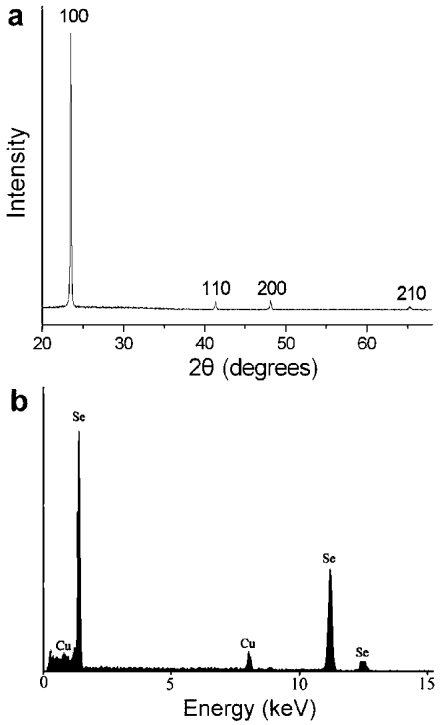

Figure 2. XRD pattern (a) and EDS spectrum (b) of Se nanobelts obtained in $C_{18}EO_{20}$ micellar solution.

grown along the [001] direction with the top surface and the side surface corresponding to the (1$\bar{1}$0) and (110) crystallographic planes, respectively. The HRTEM image shown in Figure 1f exhibits clear fringes with spacings corresponding to the (001) and (110) planes of t-Se, confirming that the obtained nanobelts are single crystals grown along the *c* axis with the top surface of the (1$\bar{1}$0) plane.

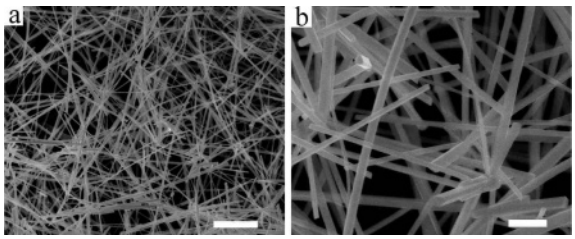

Figure 3. SEM images of Se nanowires obtained in $C_{12}EO_{10}$ micellar solution. Scale bars: (a) 5 μm and (b) 1 μm.

When the $C_{18}EO_{20}$ surfactant was replaced by another nonionic surfactant with shorter alkyl and poly(oxyethylene) chains, $C_{12}EO_{10}$, t-Se nanowires instead of nanobelts can be produced under similar synthesis conditions (Figure 3). As shown in Figure 3a, the product consists of Se nanowires with lengths ranging from several micrometers to more than 100 μm. An enlarged SEM image (Figure 3b) shows that the obtained nanowires are typically 80−400 nm in diameter and they usually adopt a prismlike morphology with a pseudohexagonal cross section. Our further experiments have shown that when the surfactant concentration is considerably changed Se nanobelts and nanowires are still the predominant products obtained in $C_{18}EO_{20}$ and $C_{12}EO_{10}$ micelles, respectively. Considering that t-Se nanotubes have been readily synthesized in $C_{12}EO_{23}$ micellar solutions,[15a] the present result suggests that the morphology of 1D t-Se nanostructures obtained in nonionic micellar solutions can be adjusted among nanobelts, nanowires, and nanotubes simply by selecting appropriate nonionic surfactants.

Although the formation of 1D t-Se nanostructures in micellar solutions can be generally attributed to the highly anisotropic structure of trigonal selenium, the exact mechanism for the selective formation of nanobelts, nanowires, and nanotubes is still under investigation. It has been proposed that the extended polar shell of nonionic micelles, which is filled with poly(oxyethylene) chains and entrapped water, may have a good ability to solubilize amorphous selenium (a-Se), the precursor for crystalline t-Se, and thereby play an important role in controlling the distribution of a-Se in the solution.[15a] It was noted that in the absence of nonionic micelles the reaction solution became brown and cloudy immediately after the addition of Na_2SeSO_3, resulting in the formation of t-Se products with irregular morphologies, which strongly indicated that nonionic micelles indeed played a role in solubilizing a-Se and brought about a gradual transformation from a-Se to t-Se under the subsequent sonication treatment. In $C_{12}EO_{23}$ micellar solutions with a suitable $C_{12}EO_{23}$ concentration, a large amount of a-Se is solubilized in the thick polar shell of the micelles, resulting in a relatively small amount of a-Se colloids in the solution. The growth of t-Se nanowires through a solid−solution−solid process would be considerably limited, and the continuous addition of Se atoms to the t-Se seeds would preferentially occur at the circumferential edges of hexagonally or trigonally facetted seeds, leading to the formation of t-Se nanotubes. Compared with $C_{12}EO_{23}$, both $C_{12}EO_{10}$ and $C_{18}EO_{20}$ are more hydrophobic because $C_{12}EO_{10}$ has the same hydrophobic hydrocarbon moiety but a shorter hydrophilic poly(oxyethylene) moiety whereas $C_{18}EO_{20}$ has a longer hydrophobic moiety and a slightly shorter hydrophilic moiety. It is expected that both $C_{12}EO_{10}$ and $C_{18}EO_{20}$ micelles have thinner polar shells consisting of poly(oxyethylene) chains and entrapped water. Therefore, a relatively small amount of a-Se can be solubilized in the micelles, and hence the formation of t-Se nanotubes is unfavorable, leading to the formation of 1D solid t-Se nanostructures such as nanowires and nanobelts. Compared with $C_{12}EO_{10}$ micelles, $C_{18}EO_{20}$ micelles are much larger with a larger nonpolar core and a thicker polar shell, which would result in a slower diffusion rate of the micelles carrying solubilized a-Se. It is noted that 1D trigonal tellurium (t-Te) nanostructures with various morphologies (e.g., blade-shaped whiskers and hexagonal needles) have been produced by adjusting the mobilities of Te species in solution, and it has been suggested that relatively low mobilities of Te species could lead to deviations from morphologies with the hexagonal cross sections expected for a perfect crystal structure of t-Te.[16] Moreover, on the basis of the hydrothermal synthesis of t-Te nanobelts, it has been proposed that an appropriately slow addition rate of tellurium atoms in solution may be helpful for the preferential growth of t-Te nanobelts grown along the [001] direction with the top surface of the $(1\bar{1}0)$ plane.[5e] Therefore, it can be reasonably speculated that in the current situation $C_{18}EO_{20}$ micelles, the larger a-Se-containing micelles with a lower diffusion rate, would favor the preferential growth of $(1\bar{1}0)$-bound t-Se nanobelts whereas the smaller $C_{12}EO_{10}$ micelles would favor the formation of t-Se nanowires with pseudohexagonal cross sections. Generally, the presence of micelles with polar poly(oxyethylene) shells may greatly influence the distribution and diffusion of selenium species in the solution, which would exert delicate control over the dynamic crystal growth process of t-Se, thereby controlling the morphology of the final 1D t-Se nanostructures. However, our present understanding

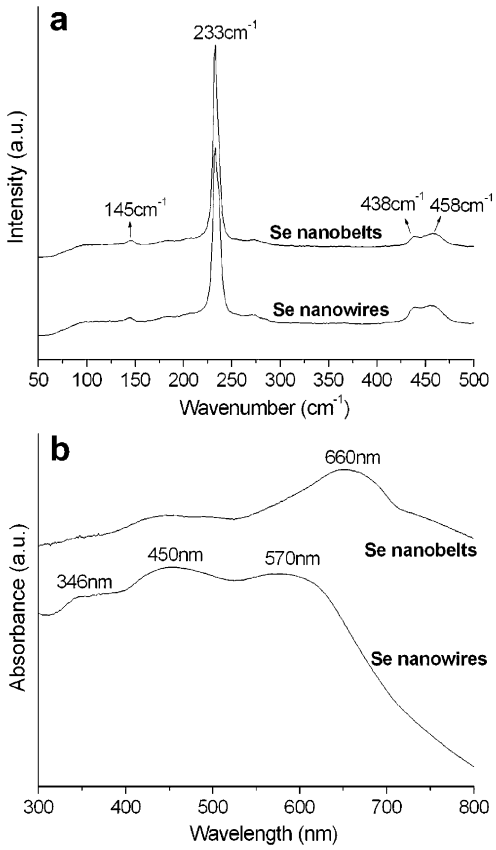

Figure 4. Raman scattering (a) and UV−vis absorption (b) spectra of Se nanobelts obtained in $C_{18}EO_{20}$ micellar solution and Se nanowires obtained in $C_{12}EO_{10}$ micellar solution.

(16) Mayers, B.; Xia, Y. *J. Mater. Chem.* **2002**, *12*, 1875.

of the morphological control of 1D t-Se nanostructures is still limited, and more in-depth studies are needed.

The t-Se nanobelts and nanowires obtained from micellar solutions have been further characterized by Raman scattering and UV−vis absorption spectra (Figure 4). As shown in Figure 4a, the Raman scattering spectra of both the Se nanowires and nanobelts are very similar and show resonance peaks characteristic of trigonal selenium (i.e., a resonance peak around 233 cm^{-1} attributed to the vibration of helical selenium chains, a peak around 145 cm^{-1} attributed to the transverse optical photon mode, and two peaks around 438 and 458 cm^{-1} attributed to the second-order modes of t-Se[17]). However, a remarkable difference can be observed in the optical absorption spectra obtained from the aqueous dispersions of the t-Se nanowires and nanobelts (Figure 4b). Three absorption peaks appear at 570, 450, and 346 nm in the absorption spectrum of the Se nanowires obtained in $C_{12}EO_{10}$ micelles, which is in good agreement with the absorption peaks at 590, 452, and 354 nm observed for the t-Se nanowires obtained by sonication of a-Se in ethanol.[10b] It is worth noting that peaks above 530 nm can be solely attributed to interchain interactions perpendicular to the *c* axis within a given t-Se crystal, hence the position of the low-energy peak at high wavelength may provide instructive information for the interchain interactions as well as the degree of crystal perfection.[10b] Interestingly, the low-energy peak is considerably redshifted to 660 nm for the t-Se nanobelts obtained in $C_{18}EO_{20}$ micelles, indicating that the interchain interactions within the nanobelts are obviously weaker than those within the nanowires. This result can be rationalized by considering that for the trigonal phase of selenium the nanowires with pseudohexagonal cross sections would have a higher degree of perfection compared with the nanobelts with rectangular cross sections. These results have revealed the morphology-dependent optical absorption characteristics of 1D t-Se nanostructures and suggest that UV−vis absorption spectra could be applicable to distinguish between t-Se nanobelts and nanowires whereas Raman scattering spectra are not useful for this purpose.

In summary, selective synthesis of single-crystalline nanobelts and nanowires of trigonal selenium in micellar solutions has been readily realized by selecting suitable nonionic surfactants with adjusted alkyl and poly(oxyethylene) chains. This facile, low-temperature, solution-phase approach to the morphology-controlled synthesis of 1D nanostructures may be potentially extended to other functional materials with highly anisotropic structures. The obtained t-Se nanobelts exhibit optical absorption characteristics quite different from those of t-Se nanowires, and they may provide an ideal system for the investigation of morphology-dependent properties and for various applications including nanodevice fabrication.

Acknowledgment. This work is supported by NSFC (20325312, 20473003, 20233010) and FANEDD (200020).

LA050801L

(17) Lucovsky, G.; Mooradian, A.; Taylor, W.; Wright, G. B.; Keezer, R. C. *Solid State Commun.* **1967**, *5*, 113.